Received: 4 November 2021 | Revised: 18 May 2022 | Accepted: 31 May 2022

DOI: 10.1111/maec.12715

RESEARCH ARTICLE

marine ecology WILEY

Evidence of increased mussel abundance related to the Pacific marine heatwave and sea star wasting

Sarah B. Traiger[1] | James L. Bodkin[1] | Heather A. Coletti[2] | Brenda Ballachey[1] | Thomas Dean[3] | Daniel Esler[1] | Katrin Iken[4] | Brenda Konar[4] | Mandy R. Lindeberg[5] | Daniel Monson[1] | Brian Robinson[1] | Robert M. Suryan[5] | Benjamin P. Weitzman[6]

[1]U.S. Geological Survey Alaska Science Center, Anchorage, Alaska, USA

[2]National Park Service, Inventory & Monitoring Program, Fairbanks, Alaska, USA

[3]Coastal Resources Associates, Inc., Carlsbad, California, USA

[4]College of Fisheries and Ocean Sciences, University of Alaska Fairbanks, Fairbanks, Alaska, USA

[5]NOAA Alaska Fisheries Science Center, Auke Bay Laboratories, Juneau, Alaska, USA

[6]U.S. Fish and Wildlife Service, Marine Mammals Management, Anchorage, Alaska, USA

Correspondence
Sarah B. Traiger, U.S. Geological Survey Alaska Science Center, 1910 Alex Holden Way, Juneau, AK 99801, USA.
Email: straiger@usgs.gov

Funding information
Exxon Valdez Oil Spill Trustee Council; U.S. Geological Survey

Abstract

Mussels occupy a key middle trophic position in nearshore food webs linking primary producers to predators. Climate-related environmental changes may synergistically combine with changes in predator abundance to affect intertidal ecosystems. We examined the influence of two major events on mussel (*Mytilus trossulus*) abundance in the northern Gulf of Alaska: the recent Pacific marine heatwave (PMH, 2014–2016) and an outbreak of sea star wasting (SSW). We investigated how mussel abundance changed since the onset of SSW and whether the density of predatory sea stars or PMH-related temperature metrics explain variation in mussel abundance. Sea stars and mussels were surveyed since 2005 approximately annually in four regions of the northern Gulf of Alaska: Katmai (KATM), Kachemak Bay (KBAY), Kenai Fjords (KEFJ) and western Prince William Sound (WPWS). Mussel percent cover in the mid-intertidal increased 1–3 years after declines in sea stars at all regions and in the low-intertidal at KATM, KBAY, and KEFJ, but not at WPWS. After the onset of SSW, large (≥20 mm length) mussel density and mussel bed width increased at KATM but not the other regions. Total mussel densities, including recruits, did not differ before and after the onset of SSW. The total number of sea stars significantly explained variation in mussel metrics, but the proportions of the three sea star species examined did not. We did not find strong evidence for direct effects of temperature on mussels. The effects of the PMH and the SSW outbreak appear to have combined, with increased temperatures indirectly benefiting mussels in concert with relaxed top-down pressure from sea stars, allowing for increased mussel abundance. Changing mussel abundance may affect intertidal local productivity and the abundance or performance of other nearshore consumers of mussels.

KEYWORDS
Evasterias troschelii, marine heatwave, *Mytilus trossulus*, *Pisaster ochraceus*, *Pycnopodia helianthoides*, sea star wasting

1 | INTRODUCTION

Intertidal communities are important for nearshore ecosystems as they provide recreational and subsistence food for humans (Harley et al., 2020; Krylovich et al., 2019) and prey for numerous other nearshore consumers (Suchanek & Seed, 1992) such as sea otters (*Enhydra lutris*), sea ducks, and sea stars (O'Clair & O'Clair, 1998). Mussels (*Mytilus* spp.) play an important role in linking primary producers to upper trophic predators and compete with other intertidal primary space holders, with consequences for productivity and biodiversity. For example, *Mytilus edulis* can outcompete intertidal seaweeds, forming extensive mussel beds (Lubchenco & Menge, 1978). *Mytilus californianus* beds provide habitat for more than 300 species (Suchanek, 1992). Although *M. trossulus* is ephemeral in locations where its competitive superior, *M. californianus* dominates, *M. trossulus* outcompetes small barnacles (Berlow, 1997), and in Alaska can form beds that persist for several years to decades (authors' personal observations). *Mytilus* spp. are globally ubiquitous, occupying the intertidal on most continents, and are model organisms for physiological and ecological processes and often used as bioindicators of pollution (Suchanek & Seed, 1992). Sea stars often act as keystone predators in the intertidal, with their predation on mussels facilitating the persistence of other habitat-forming species such as macroalgae and, thus, increasing intertidal biodiversity (Paine, 1974).

In recent years, two major events had the potential to influence mussels and the wider nearshore ecosystem. First, the Pacific marine heatwave (PMH, 2014–2016) was associated with unprecedented positive water temperature anomalies and major disruptions to marine food webs (Suryan et al., 2021). Elevated temperatures during heatwaves can affect mussel abundance through changes in metabolic rates, stress, and mortality. When adequate food is available, increased water temperature within their thermal tolerance window can increase mussel growth rates (Almada-Villela et al., 1982; Zippay & Helmuth, 2012). Both exceptionally high and low air temperatures have been shown to negatively affect *Mytilus* survival, physiology, and performance (Aarset, 1982; Carroll & Highsmith, 1996; Olabarria et al., 2016). *Mytilus trossulus* produces heat shock proteins between 23 and 28°C depending on the season in Puget Sound (Buckley et al., 2001). Numerous studies have shown elevated mortality of *Mytilus* spp. as a result of freezing air temperatures, particularly when associated with exceptionally low tides and prolonged air exposure (Bourget, 1983; Carroll & Highsmith, 1996; Davenport & Davenport, 2005; Williams, 1970).

Second, sea star populations in rocky intertidal habitats along the eastern Pacific coastline were impacted by an outbreak of sea star wasting syndrome (SSW) (Hamilton et al., 2021; Hemery et al., 2016). The SSW outbreak led to large declines in sea star populations and there is also some evidence of SSW-related declines in sea star abundance affecting sea star prey species (Cerny-Chipman et al., 2017; Gravem & Morgan, 2017). The SSW outbreak began along the west coast of North America in 2013 and affected more than 20 species (Hewson et al., 2014; http://www.seastarwasting.org). The epidemic started in Washington and California in 2013, and spread to Baja California and Alaska (Hewson et al., 2014; Miner et al., 2018). SSW reached Alaska last, with major sea star declines first observed in 2014 in the eastern Gulf of Alaska (Konar et al., 2019).

The eastern Pacific rocky intertidal community has been affected in various ways by declines in sea star abundance. Declines in *Pisaster ochraceus* during the recent SSW outbreak in Oregon led to increased abundance of small whelks, *Nucella* spp., which are preyed on by *P. ochraceus* (Cerny-Chipman et al., 2017). Populations of the black turban snail *Tegula funebralis* in northern California more than doubled and small and medium-sized individuals shifted their distribution lower in the intertidal after declines in *P. ochraceus* and *Leptasterias hexactis* due to SSW (Gravem & Morgan, 2017). In Oregon, sea star predation on mussels was up to 15.5 times lower after SSW in 2014 than for the previous 23 years (Menge et al., 2016). In some cases, despite the large decline in predation pressure due to SSW, effects on prey species were muted due to low recruitment (Cerny-Chipman et al., 2017).

To investigate potential effects of a major heatwave and a widespread sea star die-off on the abundance of Pacific blue mussels, *M. trossulus* (Gould, 1850), we used data from a long-term monitoring program in the northern Gulf of Alaska (https://gulfwatchalaska.org/monitoring/nearshore-ecosystems-4/; U.S. Geological Survey & National Park Service, 2022; U.S. Geological Survey Alaska Science Center & National Park Service Southwest Alaska Inventory and Monitoring Network, 2022; U.S. Geological Survey Alaska Science Center, National Park Service Southwest Alaska Inventory and Monitoring Network, & University of Alaska Fairbanks College of Fisheries and Ocean Sciences, 2022) that include *in situ* temperature monitoring at 20 sites where mussel and sea star abundance are surveyed annually. Our research questions were: (1) did mussel abundance change after SSW?, and (2) which sea star and temperature metrics explain variation in mussel abundance? This study demonstrates how multiple large scale disturbances can lead to large changes in mussels, which may have implications for higher trophic levels.

2 | MATERIALS AND METHODS

Intertidal temperature, sea star and mussel abundance were examined at four regions in the northern Gulf of Alaska: Katmai National Park and Preserve (KATM), Kachemak Bay (KBAY), Kenai Fjords National Park (KEFJ), and western Prince William Sound (WPWS, Figure 1). Some differences in methods between KBAY and the other regions exist because two separate, historic monitoring programs were merged into the Gulf Watch Alaska program. However, comparative analyses have shown that data are comparable among regions (Konar et al., 2016) and are further discussed in syntheses of data from across the northern Gulf of Alaska (Konar et al., 2019; Weitzman et al., 2021). Five sites were sampled in each region (Table S1). Rocky sites in KBAY were selected to be similar in slope, substrate, and exposure and have at least 100 m of continuous rocky

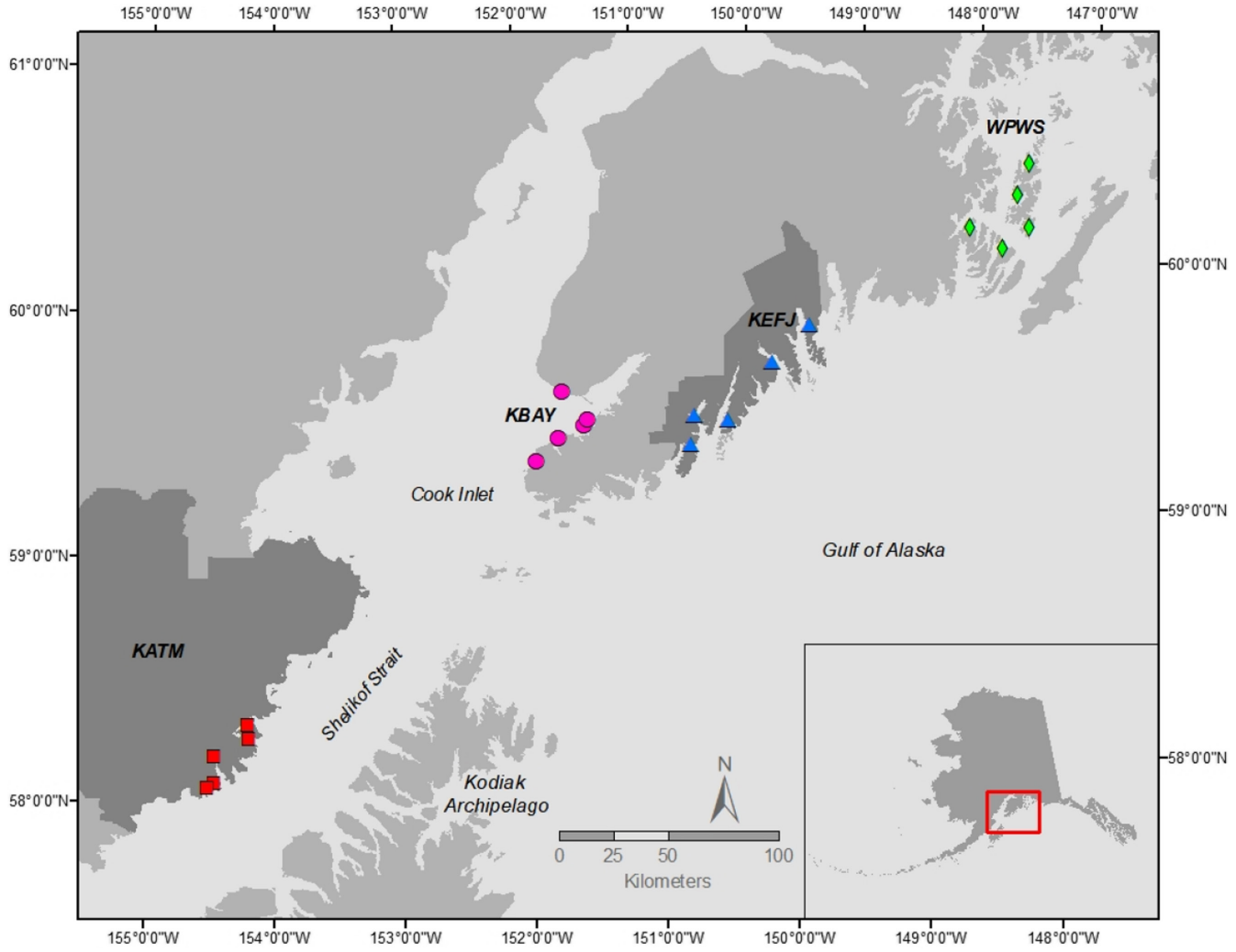

FIGURE 1 Map of study area showing locations of study sites within each of the four regions (Katmai National Park and Preserve (KATM), Kachemak Bay (KBAY), Kenai Fjords National Park (KEFJ) and western Prince William Sound (WPWS))

habitat. Rocky sites in the other three regions were selected using generalized random tessellation stratified sampling from maps of sheltered rocky shoreline (Dean et al., 2014). At KATM, KEFJ, and WPWS, mussel bed sites were defined as the closest 100 m of contiguous mussels to the rocky site. In KBAY, mussel bed sites were directly adjacent to each rocky site. At KATM, KEFJ, and WPWS the mussel bed sites are often not at the exact same location as the rocky sites but are in close proximity (within 4.1 km). Here we refer to the rocky and mussel bed locations as one site. For more details on rocky site and mussel bed locations, see Table S1. Mussel and sea star abundance have been monitored approximately annually starting in 2005 (see Table S1 in the Supporting Materials for details on data availability in each year and region).

2.1 | Temperature

To monitor intertidal temperature, HOBO V2 temperature loggers (Onset Computer Corporation, Bourne, MA, USA) were placed at each rocky site (U.S. Geological Survey Alaska Science Center, National Park Service Southwest Alaska Inventory and Monitoring Network, & University of Alaska Fairbanks College of Fisheries and Ocean Sciences, 2022). Loggers were installed in 2007 at KATM and KEFJ, in 2010 at WPWS, and 2013 at KBAY (Table S1). The HOBO temperature sensors had measurement accuracy of ±0.2°C. Loggers were placed inside a 1.5-inch diameter PVC pipe, which was bolted to a boulder or bedrock at 0.5 m above mean lower low water (MLLW). Loggers recorded temperature every 20, 30, or 60 min. Prior to 2013 logger sampling frequency was inconsistent: from 2013–2017 loggers were mostly set to record every 60 min, and since 2018, loggers have consistently been set to record every 30 min. Data were separated into water temperature when the tide level from the nearest tide station was ≥1.5 m (logger wet) and air temperature when the tide was ≤0 m (logger dry; Tides and Currents software, NOBELTEC, Beaverton, OR, USA). Transition periods when it was unclear whether the loggers were submerged were omitted. Temperatures were averaged within five time periods relating to mussel life history: late winter (January–March, gonad development), spring

(April–May, spawning and settlement), summer (June–July, spawning and early growth), fall (August–October, spawning and late growth), and early winter (November–December, senescence and early gonad development; Suchanek & Seed, 1992, Blanchard & Feder, 1997, Hiebert, 2016). Water temperature anomalies were calculated by subtracting logger mean seasonal water temperatures from the regional mean for the whole time series within each of the five time periods (Figure S1).

Hours of exposure to extreme warm (≥25°C) and cold (≤−4°C) air temperatures from HOBO loggers at each site were summed for each day and averaged within above-mentioned five time periods. These air temperatures fall outside of the average maximum air temperature in summer and average minimum air temperature in early and late winter (Figure S2). Air temperature metrics were based on absolute temperatures rather than anomalies because air temperatures are more variable than water temperatures and can more easily exceed the physiological limits of intertidal mussels.

Air temperature close to the rock surface where mussels live in the rocky intertidal can be highly influenced by aspect and topography that can affect shading. To assess air temperature variability within sites, we examined one year of temperature data when an additional logger was placed at the end of the +0.5 m MLLW transect at two sites and an additional logger was placed at the start of the transect at one mussel site. For hours of exposure to extreme air temperatures, the largest difference between the start and end of the rocky transect was 0.06 h (3.6 min) for warm air temperatures and 0.03 h (1.8 min) for cold air temperature (Figure S3). These differences are small compared to the overall range of values (0–4.25 h cold air exposure, 0–3.5 h of warm air exposure) and are unlikely to be biologically relevant, so we considered these measurements of the single 0.5 m logger at other sites and across years representative and included them in our analysis. However, maximum and minimum air temperature varied by several degrees between the start and end of the rocky transect and between the rocky site and mussel bed site (Figure S3), so we did not include maximum and minimum air temperature in our analysis.

2.2 | Sea stars

Sea star species that consume mussels (*Evasterias troschelii*, *Pisaster ochraceus*, and *Pycnopodia helianthoides*, Table S1 [Herrlinger, 1983; Kay et al., 2019; Mauzey et al., 1968; O'Clair & Rice, 1985; Paul & Feder, 1970; Sewell & Watson, 1993]) were counted annually at low tide along transects in the low intertidal at rocky sites to estimate their density (U.S. Geological Survey & National Park Service, 2022). Individuals of all sizes were counted. *Leptasterias* spp. also consume mussels but are not counted in the Gulf Watch Alaska long-term monitoring program because of their cryptic behavior, although they can be abundant at some sites (authors' personal observations). For survey details see Konar et al. (2019) and Dean et al. (2014). Sea star densities were calculated and are presented here as individuals per 200 m^{-2}. Pre- and post-SSW periods were defined for each region based on when sea stars with SSW were first observed (Konar et al., 2019). At KATM, SSW was only observed in individuals off transect; however, there was a large decline in sea star density after 2016 (Konar et al., 2019), so the pre-SSW period was defined as 2006–2016 and post-SSW as 2017–2019.

2.3 | Mussels

Several different metrics of mussel abundance were used to assess the response of mussels to changing sea star density with SSW (Bodkin et al., 2016; Dean et al., 2014; U.S. Geological Survey, & National Park Service, 2022; U.S. Geological Survey Alaska Science Center & National Park Service Southwest Alaska Inventory and Monitoring Network, 2022). Percent cover of mussels was estimated at 0.5 and 1.5 m above MLLW at rocky sites. Percent cover was either estimated visually (KBAY) or by proportion of points occupied by mussels (KATM, KEFJ, WPWS) within twelve 0.25 m^2 quadrats randomly placed along 50-m transects at each of the two tide heights (Dean et al., 2014). Mussel densities, sizes, and bed width were measured on 10 randomly placed transects or quadrats within mussel bed sites. As data for these metrics were collected across the whole vertical extent of mussel beds, they cover a wider elevation range than mussel percent cover, which was limited to 0.5 and 1.5 m above MLLW. Mussels were collected and measured to the nearest mm. At KBAY all mussels ≥2 mm were collected from ten 0.0625 m^2 quadrats. At KATM, KEFJ, and WPWS mussels ≥20 mm were collected from ten variable sized quadrats (sized to contain at least 20 individuals) and 51-mm interior diameter cores (0.0021 m^2) were collected to count all mussels ≥2 mm. To determine mussel bed width, 10 random transects were placed perpendicular to a fixed baseline transect that bisected the mussel bed. Mussel bed width was measured at each of these points and averaged. The contiguous mussel bed was defined by the absence of mussels below a strip 12 mm wide by >1 m long. For more details see Bodkin et al. (2016).

2.4 | Data analysis

To test for differences before and after SSW among regions, linear mixed effect models were used for density of each sea star species and each metric of mussel abundance in R (R Core Team, 2020) using the lme4 package (Bates et al., 2015). Box-Cox transformations were used for each variable. Fixed factors included SSW (2 levels: pre-SSW, post-SSW) and region (4 levels: KATM, KBAY, KEFJ, WPWS). Site was included as a random factor. The model formula used was: $((x+0.1)\text{^}b) \sim \text{SSW}^* \text{ Region} + (1|\text{Site})$, where x is the sea star species or mussel metric and b refers to the Box-Cox transformation value.

PERMANOVA tests were used in the multivariate statistical software package, PRIMER (v6, Plymouth Marine Laboratories, Anderson et al., 2008) to test for the effects of temperature metrics and sea star abundance on the multivariate mussel metric data, after accounting for effects of region, site, and year. For all PERMANOVA

tests, the multivariate mussel data were log(*x*+1) transformed to reduce right skew and a Euclidian distance matrix was calculated, 9999 permutations were used, and we used Type I sum of squares. We first tested for the effects of site, region, pre- and post-SSW, and year: Mussels ~ Region + Site(Region) + SSW + Year, with region, site, and year as random factors and SSW as a fixed factor.

Next, we tested for the effects of temperature on mussel metrics after accounting for the effects of region, site, SSW, and year. Temperature data paired with mussel metrics spanned approximatley the 12 months prior to mussel sampling. Since exposure to warm and cold air temperature metrics were right-skewed, we log(*x*+1) transformed the data and used a Gower similarity matrix to create a metric multidimensional scaling (mMDS) plot. We used the two mMDS axes to reduce the six air temperature exposure variables (cold air exposure in late winter, spring, and early winter, warm air exposure in spring, summer, and fall). The first mMDS axis (AirTempExposuremMDS1) represented a continuum from exposure to cold air to warm air in spring, summer and fall, and the second mMDS axis (AirTempExposuremMDS2) represented a continuum from low to high exposure time to cold air in early and late winter (Figure 2a). To reduce the ten water temperature metrics (mean water temperature and water temperature anomaly in each of the five seasons), we used the two axes from a principal component analysis (PCA). The first PCA axis (WaterTempPCA1, 58.4% of variation) represented a continuum from low mean water temperature and negative anomaly to warmer mean water temperature and positive anomalies (Figure 2b). The second PCA axis (WaterTempPCA2, 20.2% of variation) represented differences in water temperature in summer among regions (Figure 2b). To test for the effects of temperature on mussel metrics we used a PERMANOVA with Mussels ~ Region + Site(Region) + SSW + Year + AirTempExposuremMDS1 + AirTempExposuremMDS2 + WaterTempPCA1 + WaterTempPCA2. We also ran the PERMANOVA with the water temperature PCA axes listed before the air temperature mMDS axes.

Next, we tested for effects of sea stars on the mussel metrics after accounting for the effects of region, site and year. We summed the densities of the three sea star species for each site and year to calculate total sea star density. We then converted the densities of the three sea star species to proportions by standardizing by the total number of stars. We used a PCA analysis to reduce the three sea star proportion variables to two PCA axes, the first representing proportion of *P. ochraceus* and *P. helianthoides* (StarsPCA1, 47.8% of variation) and the second representing proportion of *E. troschelii* (StarsPCA2, 35.2% of variation, Figure 2c). To test for the effects of sea stars on mussel metrics we used a PERMANOVA

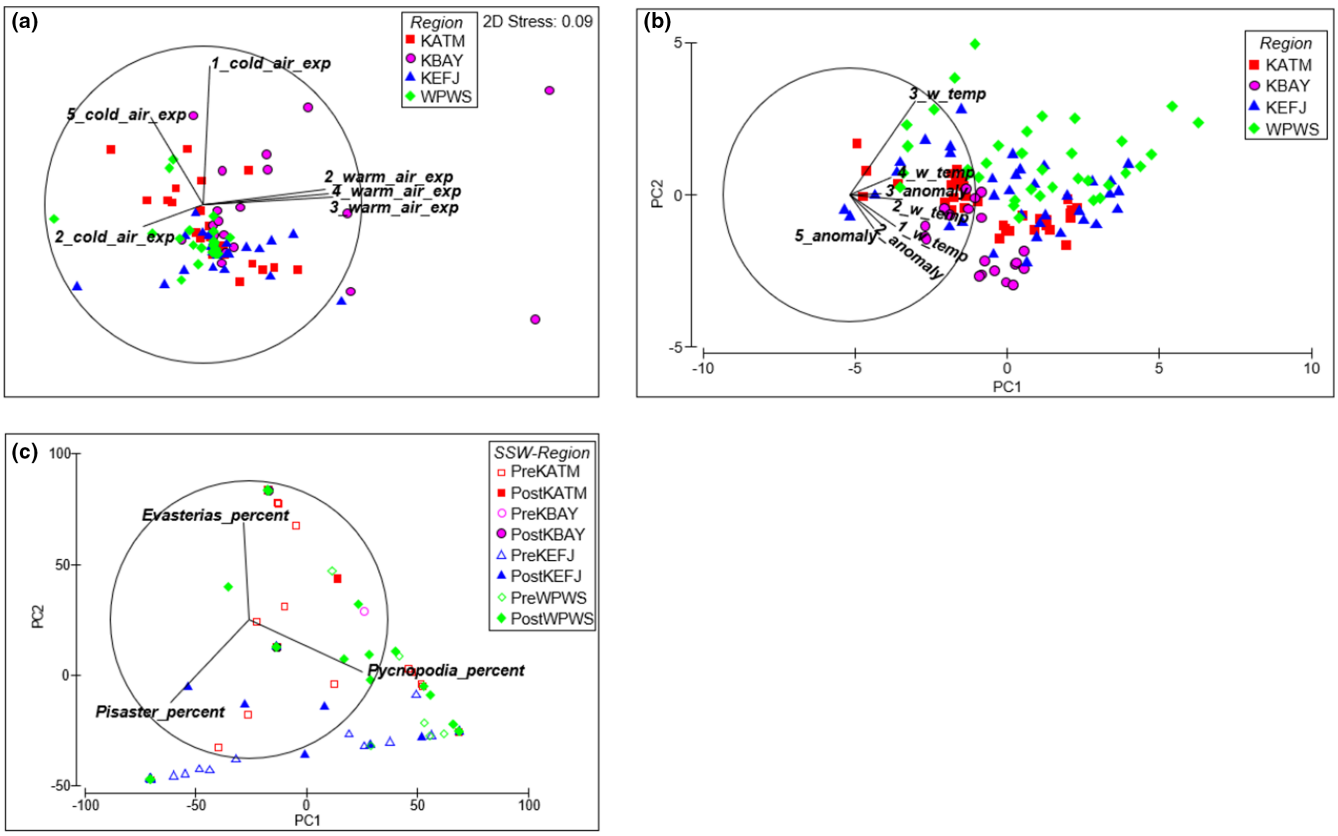

FIGURE 2 Analyses used to reduce covariates for the PERMANOVA tests of mussel metrics. In each panel data points are color coded by region (KATM = red, KBAY = pink, KEFJ = blue, WPWS = green). Vectors indicate the influence of each variable on the placement of data points within the plot. (a) Metric-MDS plot of mean daily exposure to warm air (≥ 25°C), cold air (≤ -4°C) temperature metrics in each season (1: late winter, 2: spring, 3: summer, 4: fall, 5: early winter). (b) PCA of water temperature metrics from each season. (c) PCA of proportions of each of the three sea star species. Open symbols are pre-SSW and closed symbols are post-SSW

with Mussels ~ Region + Site(Region) + SSW + Year + Total Stars + StarsPCA1 + StarsPCA2.

3 | RESULTS

3.1 | Temperature trends across the northern Gulf of Alaska

Starting in 2013–2014, the Gulf of Alaska was affected by a marine heatwave and water temperature in all regions had positive anomalies for an extended period (Figure 3). In KATM, water temperature anomalies increased above zero in 2014 and persisted for all seasons through 2016 (Figure 3). At KEFJ and WPWS, water temperature anomalies increased above zero starting in spring 2014 and remained positive through spring 2017 in KEFJ and late winter 2017 in WPWS (Figure 3). KBAY differed from the other regions in that water temperature anomalies increased above zero in fall 2014, and remained positive through early winter 2016, except for fall and early winter 2015 (Figure 3). There were also positive water temperature anomalies in 2019, with summer water temperature anomalies at KEFJ and WPWS exceeding those observed during the 2014–2016 heatwave (Figure 3). Mean water temperature was similar among regions but tended to be higher at WPWS (8.5 ± 3.4°C, mean of whole time series across all sites ± sd) and KEFJ (8.0 ± 3.0°C) than at KBAY (7.5 ± 2.6°C) and KATM (7.3 ± 3.1°C) (Figure S1). During years when there was overlap in data across all regions, summer water temperature was frequently >2.5°C higher at WPWS than at KBAY (Figure S1).

Mean hours of exposure to low (≤ −4°C) and high (≥ 25°C) air temperatures varied among regions and seasons (Figure 3). Mean exposure to low air temperatures tended to be less during the PMH (Figure 3). The highest mean exposure to high air temperature (1.9 h) occurred in KEFJ in summer 2008. Mean exposure to high air temperature was also high in KATM in summer 2006 and 2007. During the PMH (2014–2016), mean exposure to high air temperature was highest during the summers in KBAY where mean exposure was 1.2–1.3 h (Figure 3). Mean exposure to high air temperature was low throughout the time series at WPWS (Figure 3).

3.2 | Decline in sea stars with SSW

Before the onset of SSW, there were some differences in densities of *Evasterias troschelii*, *Pisaster ochraceus*, and *Pycnopodia helianthoides* among regions (Tables 1, S4 and S5). While all species occurred in all regions, the most abundant mussel-preying sea star was *E. troschelii* at KATM and KBAY, *P. ochraceus* at KEFJ, and *P. helianthoides* at WPWS. Although there was a significant decline post-SSW of at least one species in each region, KEFJ and WPWS retained more mussel-preying sea stars post-SSW than KATM and KBAY. At KATM all three sea star species declined significantly by 87–96% (Table 1). At KBAY there was a 100% decline in *E. troschelii*. *Pisaster ochraceus* and *P. helianthoides* were so rare before SSW at the study sites that even their absence post-SSW was not statistically significant (Table 1). At KEFJ and WPWS, there was a significant decline, by 53% and 67% respectively, in mean density of *P. helianthoides* after SSW (Table 1).

3.3 | Variation in mussel abundance and relationships to temperature and sea stars

Differences in mussels pre-and post-SSW were mostly driven by increases in percent cover. In univariate analyses, mussel percent cover at 0.5 m was significantly higher post-SSW at KATM, KBAY, and KEFJ, but not WPWS, and mussel percent cover at 1.5 m was significantly higher post-SSW at all regions (Tables 1, S6). Large mussel density only significantly increased at KATM (Tables 1, S6). Total mussel density was not significantly different pre- and post-SSW in any region (Tables 1, S6). Mussel bed width only significantly increased at KATM (Tables 1, S6). The multivariate cloud of mussel metrics varied significantly among sites nested within regions, pre- and post-SSW, and among years, but not among regions (Table 2, Figure 4a). Vectors on the nMDS plot indicate the direction of influence of each mussel metric in the placement of datapoints on the plot (Figure 4). Variation in large and total mussel density among regions is reflected in the separation of points from left to right. Pre- and post-SSW data points within each region range from the top to the bottom of the plot, following the percent cover vectors, reflecting that percent cover metrics varied pre- and post-SSW, particularly at KATM (Figure 4a).

In general, there was not a significant effect of the temperature metrics on mussel metrics after accounting for the effects of region, site SSW, and year; however, the first mMDS axis for exposure to extreme air temperature metrics (AirTempExpMDS1) was significant under certain conditions (Tables 2, S7). AirTempExpMDS1 was only significant in models where SSW was included and the water temperature PCA axes were listed before air temperature mMDS axes (Tables 2, S7). AirTempExpMDS1 represents a continuum from exposure to cold air in spring to exposure to warm air in spring, summer, and fall (Figure 2a). KBAY had higher exposure to warm air in spring, summer, and fall in many years compared to the other regions (Figures 2a, 3). Exposure to warm air temperature in spring through fall may explain some of the variation in mussel metrics between KBAY and the other regions.

After accounting for the effects of region, site, SSW, and year, there was a significant effect of total sea star density, but there was no significant effect of the PCA axes based on sea star species proportions (Table 2). The effect of total stars was small (sum of squares 10.747) compared to that of site (514.080), year (71.319), and SSW (51.761). The significance of total stars increased when SSW was not included (sum of squares 12.160, Table S8). The model with the lowest AIC included both SSW and total stars (Table S8). The nMDS plot of mussel metrics with bubbles overlaid showing total density of sea stars illustrates the effect of sea stars on mussels (Figure 4b). Points with higher percent cover of mussels and

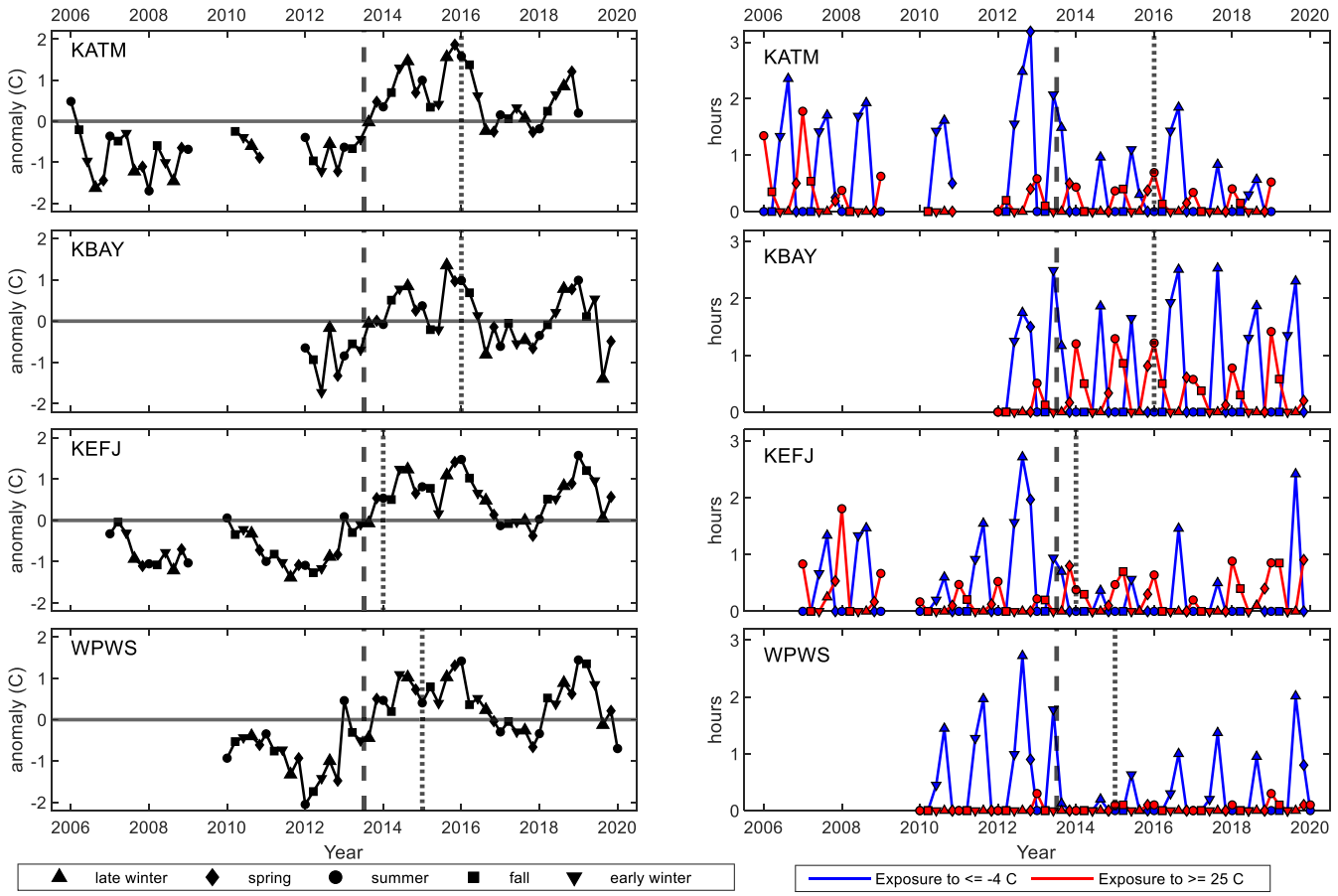

FIGURE 3 Left: Water temperature anomalies (relative to regional means) in each region (Katmai Naitonal Park and Preserve (KATM), Kachemak Bay (KBAY), Kenai Fjords National Park (KEFJ) and western Prince William Sound (WPWS)). Right: Mean daily hours of exposure to air temperature ≤ -4°C and ≥ 25°C. In all plots the vertical dashed line indicates the start of the Pacific marine heatwave and the dotted line indicates appearance of sea star wasting in each region. Shapes indicate season

higher mussel density are associated with lower sea star density, indicating that higher sea star density has a negative effect on mussel percent cover and density. In particular many of the high percent cover points coincide with low or zero density of sea stars. The upper region of the plot shows sites and years where there is low percent cover but high large mussel density. These sites and years usually had total star density < 40/200 m^2.

In most cases, increases in mussels lagged several years behind the PMH and SSW (Figure 5). At KATM, percent cover of mussels at 1.5 m, density of large mussels, and bed width all began increasing during the PMH and further increased in 2018, two years after the large decline in sea stars in 2016. Percent cover at 0.5 m did not increase as much during the PMH but also increased sharply after SSW. At KBAY, mussel metrics changed little during the PHM and mussel percent cover at 0.5 m and 1.5 m started increasing in 2018, two years after the onset of SSW. At KEFJ, mussel percent cover at 0.5 m increased sharply in 2014, followed by a decline, then began an increasing trend in 2017. Percent cover at 1.5 m increased in most years since the start of the PMH in 2014. At WPWS, percent cover of mussels at 1.5 m increased during the PMH in 2014 and remained higher than the years before the PMH through the rest of the time series.

4 | DISCUSSION

A strength of long-term monitoring is the ability to quantify changes in natural systems after unexpected events. Here we draw on the rich literature on rocky intertidal species interactions to cautiously infer the mechanisms driving the changes we observed in mussels over time. Generally, the two large-scale disturbances (SSW and PMH) appear to have benefited mussels. High water and air temperatures may have affected mussel competitors and increased available space (Weitzman et al., 2021), then the reduced predation pressure caused by SSW allowed mussels to increase in density and persist. Although absolute mussel and sea star abundances differed among regions before these disturbances, most regions showed similar patterns: sharp decline in sea star abundance after the onset of SSW, and delayed increase in mussels as shown by one or more mussel metrics, and most consistently among regions by mussel percent cover. This study shows how a foundation species that is also important in intertidal food webs can respond to large-scale biological and physical disturbances and highlights the importance of long-term monitoring for elucidating such patterns.

TABLE 1 Mean (±SE) sea star densities and mussel metrics pre- and post-sea star wasting (SSW), percent change from pre- to post-SSW, and *p*-values from the linear mixed effects models pre- and post-SSW comparisons for each region (Katmai National Park and Preserve (KATM), Kachemak Bay (KBAY), Kenai Fjords National Park (KEFJ) and western Prince William Sound (WPWS)). For sample sizes see Table S1 in the Supporting Materials. Mussel percent cover was surveyed at 0.5 m and 1.5 m above mean lower low water at rocky sites and mussel density and bed width was surveyed at nearby mussel beds

	Sea stars (× 200 m^{-2})			Mussel metrics				
	E. troschelii	*P. ochraceus*	*P. helianthoides*	0.5 m, % Cover	1.5 m, % Cover	≥ 20 mm Density (x m^{-2})	≥ 2 mm Density (× m^{-2})	Bed Width (m)
KATM								
Pre-SSW	14.9 ± 3.0	5.4 ± 1.5	5.5 ± 1.0	2.7 ± 0.7	10.0 ± 1.6	1069 ± 158	9454 ± 1359	7.1 ± 0.8
Post-SSW	1.6 ± 1.3	0.2 ± 0.2	0.7 ± 0.7	19.7 ± 4.4	31.2 ± 5.9	2332 ± 442	15,154 ± 2851	14.6 ± 3.9
% Change	−89%	−96%	−87%	+86%	+68%	+54%	+38%	+51%
P-value	**< 0.001**	**0.014**	**< 0.001**	**< 0.001**	**< 0.001**	**0.003**	0.216	**0.008**
KBAY								
Pre-SSW	11.7 ± 4.1	0.09 ± 0.07	0.3 ± 0.09	0.02 ± 0.02	0.3 ± 0.1	1068 ± 203	7042 ± 840	2.9 ± 0.2
Post-SSW	0.05 ± 0.05	0.0 ± 0.0	0.0 ± 0.0	5.7 ± 2.6	8.4 ± 3.7	1200 ± 181	7082 ± 933	6.7 ± 1.5
% Change	−100%	−100%	−100%	+100%	+96%	+11%	+0.6%	+57%
p-value	**< 0.001**	1.000	0.755	**0.002**	**0.001**	1.000	1.000	0.231
KEFJ								
Pre-SSW	1.7 ± 1.3	28.7 ± 5.3	10.0 ± 1.6	6.9 ± 14.3	15.5 ± 3.2	2583 ± 405	27,491 ± 5343	14.5 ± 1.9
Post-SSW	1.0 ± 0.6	13.0 ± 3.5	1.6 ± 0.8	14.8 ± 4.1	28.6 ± 5.4	3528 ± 906	21,038 ± 4929	12.9 ± 1.9
% Change	−41%	−55%	−84%	+53%	+46%	+27%	−23%	−11%
p-value	0.995	0.480	**< 0.001**	**0.001**	**0.023**	0.977	1.000	1.000
WPWS								
Pre-SSW	1.2 ± 0.2	0.4 ± 0.2	23.1 ± 5.9	5.3 ± 1.6	7.6 ± 2.2	329 ± 60	3162 ± 1001	6.0 ± 0.4
Post-SSW	2.4 ± 0.9	0.6 ± 0.2	8.1 ± 2.3	7.4 ± 2.1	13.3 ± 8.8	428 ± 67	3296 ± 931	5.9 ± 0.5
% Change	+50%	+33%	−67%	+28%	+43%	+23%	+4%	−2%
p-value	1.000	0.872	**< 0.001**	0.951	**0.002**	0.952	0.885	1.000

p-values < 0.05 are in bold.

4.1 | Potential combined effects of the PMH and SSW on mussels

The PMH, followed by reduced predation pressure from sea stars, likely created favorable conditions for mussels to increase, with indirect effects on mussels through effects on their competitors rather than direct physiological effects on mussels themselves. Another study using data from the Gulf Watch Alaska nearshore monitoring program found that percent cover of *Fucus distichus* and other macroalgae declined across the northern Gulf of Alaska after the PMH in the mid and low intertidal (Weitzman et al., 2021). This created open space, which was then colonized by barnacles and mussels (Weitzman et al., 2021). Mussel recruitment has been largely consistent across the northern Gulf of Alaska since 2005 (Bodkin et al., 2018, this included the same sites as this study, excluding KBAY), so settling mussels were available to take advantage of the open space left by the decline in macroalgae and by prior declines in mussel abundance. In rocky intertidal communities, bare space is typically colonized by early successional species, including barnacles and mussels, and mussels can maintain dominance until removed by physical disturbance or predation (Farrell, 1991; Sousa, 1979, 1984; Wootton, 1993). All the mussel beds surveyed in this study have persisted since monitoring began (as early as 2008 for some sites). Juvenile mussels may have grown at faster rates during the PMH, as *Mytilus* spp. growth rate increases with water temperature (3–20°C Almada-Villela et al., 1982; 17–24°C Lazo & Pita, 2012), allowing them to occupy more space quickly. The reduced sea star densities in the years following the PMH may have reduced post-recruitment mortality from predation, allowing mussels to persist in the low intertidal longer than they normally would have. It is possible that these two large-scale events acted together to produce the large observed increase in mussels.

Our study indicates that the outbreak of SSW may have led to coherent changes in mussels, particularly percent cover in the low and mid intertidal, despite regional and site-to-site variability in community structure and site physical characteristics (Konar et al., 2016; Weitzman et al., 2021). Although increases in mussel percent cover, density, and mussel bed width were evident prior to SSW at some locations, mussel metrics continued increasing post-SSW and, in KATM and KBAY, reached the highest levels observed in the time series. The regions we sampled varied by which mussel-eating sea star species was the most numerically dominant prior

TABLE 2 PERMANOVAs testing the effects of region, site within region, pre- and post-SSW, year, temperature metrics, and sea stars on mussel metrics. Significant values ($p > 0.05$) are bolded. df, degrees of freedom; SS, sum of square

Sources of variation	df	SS	Pseudo-F	*p*-value
Testing effects of region, site, SSW, year				
Region	3	217.830	2.023	0.062
Site(Region)	15	514.080	8.699	**<0.001**
SSW	1	51.761	7.264	**<0.001**
Year	10	71.319	1.833	**0.028**
Residual	93	361.790		
Total	122	1216.800		
AIC = 732.601				
Testing effects of water temperature, air temperature exposure				
Sources of variation	df	SS	Pseudo-F	*p*-value
Region	3	217.830	2.023	0.060
Site(Region)	15	514.081	8.949	**<0.001**
SSW	1	51.761	7.264	**0.001**
Year	10	71.319	1.888	**0.023**
WaterTempPCA1	1	3.313	0.877	0.441
WaterTempPCA2	1	3.668	0.971	0.393
AirTempExpMDS1	1	11.504	3.045	**0.037**
AirTempExpMDS2	1	7.050	1.866	0.123
Residual	89	336.260		
Total	122	1216.800		
AIC = 731.600				
Testing effects of sea stars				
Region	3	217.830	2.023	0.053
Site(Region)	15	514.080	8.731	**<0.001**
SSW	1	51.761	7.264	**<0.001**
Year	10	71.319	1.840	**0.024**
Total Stars	1	10.747	2.773	**0.047**
StarsPCA1	1	1.897	0.489	0.712
StarsPCA2	1	0.364	0.094	0.985
Residual	90	348.78		
Total	122			
AIC = 734.096				

to SSW but all regions had a dramatic decline in density of at least one species and our analysis indicated that total mussel-eating sea star density was more important than the identity of the species present. KEFJ and WPWS retained more sea stars post-SSW than KATM and KBAY, which may explain the relatively small change in mussels at KEFJ and WPWS. In addition, mussels are more prominent in the diet of sea otters at KEFJ and WPWS than at KATM and KBAY (Coletti et al., 2016), which may have limited the response of mussels metrics in these areas. The magnitude of the response of mussels to the sea star decline also likely depended in part on environmental factors affecting sea star abundance and predation rates, mussel recruitment, growth and survival, and the presence of other mussel predators such as sea otters, sea ducks, and predatory snails. Sea star predation rates decrease with declining water temperature (Sanford, 1999), so sea star predation pressure may be lower in colder regions, like KBAY and KEFJ (Figures 3, S1). Although individual sea star predation rates may have increased during the PMH due to increased water temperature, overall sea star predation pressure was likely low due to the reduction in sea star populations by the SSW outbreak.

Differences in how the various mussel metrics responded (or did not show a strong response) to the PMH and SSW may reflect ecological differences between the low intertidal (mussel percent cover at rocky sites) and higher elevation mussel beds (mussel density and bed width). Mussel percent cover in the low and mid intertidal may have had a greater capacity to increase in response to changes in cover of their competitors after the PMH (Weitzman et al., 2021) than in the mussel beds. Before SSW, sea stars may have had less impact on mussels in the higher elevation mussel beds, so the loss of sea stars may have had less impact there. Additionally, mussels

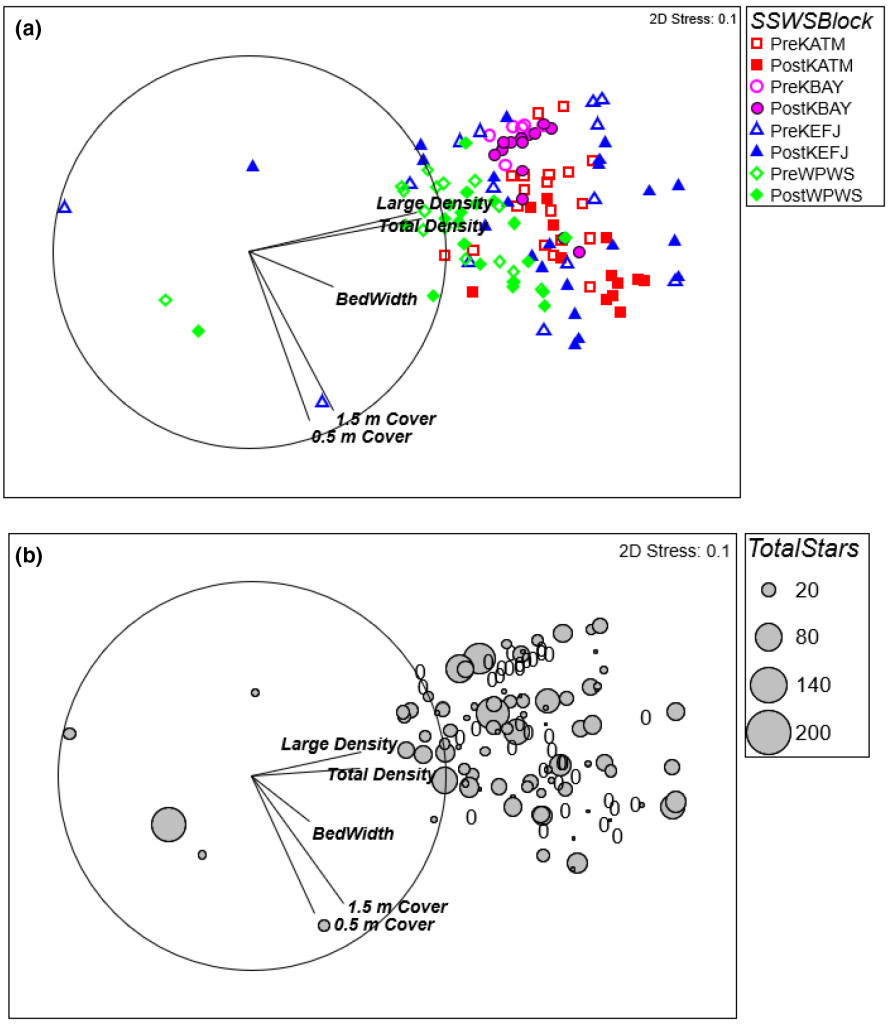

FIGURE 4 Non-metric multidimensional scaling (nMDS) plot of mussel metrics ($n = 123$). (a) Symbols correspond to pre- and post-SSW in each region. (b) Bubbles overlaid on points indicate density of sea stars. Zeros indicate that sea stars were absent. Vextors indicate the direction of influence of each mussel metric on placement of the data points

within the higher elevation mussel beds and at the upper limit of the mussel bed may be more vulnerable to higher air temperatures during the PMH than those in the low and mid intertidal, and this source of stress may have limited the increase in the mussel density and mussel bed width metrics. Differences in mussel percent cover between the low (0.5 m above MLLW) and mid (1.5 m above MLLW) tidal elevations could indicate different levels of sea star predation pressure. Mussels tend to be more abundant at higher elevations because sea stars are limited to lower elevations due to their lower desiccation tolerance (Donahue et al., 2011). At KBAY, this effect was muted as sea star density was relatively low prior to SSW and there was little difference in mussel percent cover between elevations.

4.2 | Temperature effects on mussels

Although water and air temperature has direct effects on mussel physiology (Zippay & Helmuth, 2012), we did not detect a strong direct effect of water temperature, water temperature anomaly, or mean exposure to extreme high or low air temperature on mussel metrics. The lack of significant effect of these temperature metrics on mussels could reflect (1) direct effects were masked by other factors; (2) changes in temperature during the study period remained within *M. trossulus*' tolerance window; or (3) the temperature metrics we used do not accurately reflect the conditions mussels are experiencing. Although water temperature was higher than normal during the PMH, mean seasonal water temperature remained below 14°C. Lab experiments on *M. trossulus* stress responses to heat have used treatment temperatures far above the seasonal mean temperatures during the PMH at our study sites (21–32°C) (Lockwood & Somero, 2011; Tomanek & Zuzow, 2010). A mass mortality event of *M. trossulus* occurred in British Columbia in 2021 when low tides coincided with high air temperatures and rock surfaces along the shoreline exceeded 50°C (White et al., 2022). Throughout our study period, exposure time to air temperatures ≥25°C was low and no mass mortality events were observed at our study sites. Air temperature near the substrate in the rocky intertidal is highly influenced by aspect, topography, and shading (Harley, 2008), so air temperature from HOBO loggers may not represent the exact conditions that individual mussels experience.

Marine heatwaves are expected to occur more frequently in the future (IPCC, 2019) and extreme temperatures experienced during heatwaves will likely become normal temperature conditions over the current century (Walsh et al., 2017). Increasing temperature will

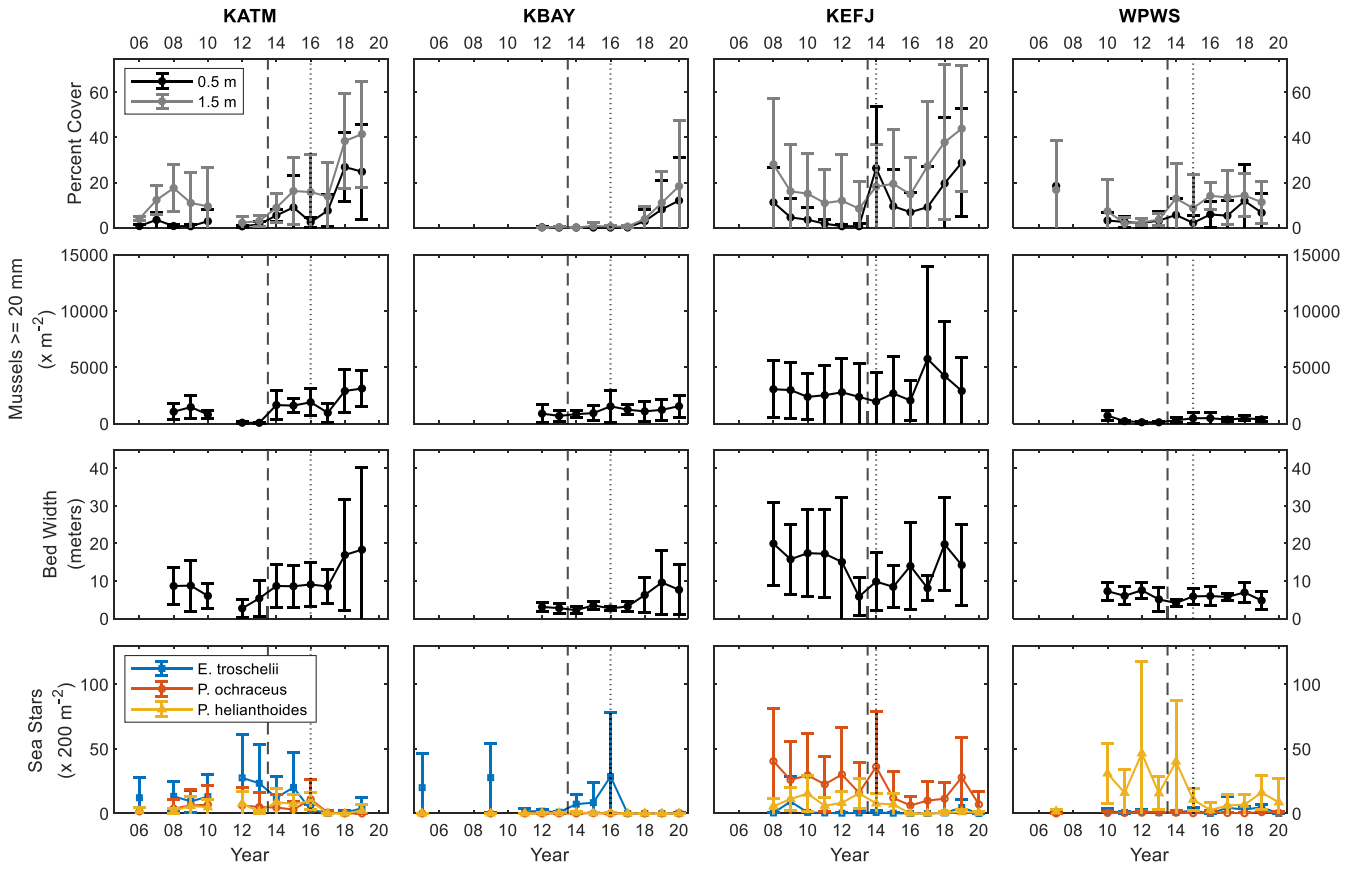

FIGURE 5 Time series of mussel percent cover, density of large mussels, mussel bed width, and sea star density in each region. Each variable is the mean (±SD) of all sites within a region ($n = 5$ in most years). The vertical dashed line indicates the start of the Pacific marine heatwave. The vertical dotted line indicates when sea star wasting appeared in the region

continue to have effects on sea stars that could affect the intertidal food web, as sea star predation rates vary across a few degrees of natural temperature variation (Sanford, 1999, 2002). Warming can affect predator–prey interactions differently in different seasons. For example, in mesocosm experiments, warm winter temperatures increased sea star metabolic rates but sea stars did not increase their feeding rates on mussels, in part because mussel body condition declined (Melzner et al., 2020). Mussels' greater resistance to high temperatures compared with some of their intertidal algal space competitors (Weitzman et al., 2021), combined with the benefits mussels may experience from increased temperature during their larval and juvenile stages (Almada-Villela et al., 1982; Rayssac et al., 2010) could enable them to maintain dominance in the intertidal as long as temperatures remain within mussel's tolerance windows. However, mussels are also susceptible to ocean acidification. Acidified conditions can lead to lower mussel recruitment and cover (Brown et al., 2016), decreased calcification (Gazeau et al., 2007), production of weaker byssal threads (O'Donnell et al., 2013), and decreased larval growth and development (Kurihara, 2008). Glacial discharge increases the corrosivity of $CaCO_3$ in surface waters (Evans et al., 2014). Understanding the direct physiological effects of environmental stressors, indirect effects on species interactions, and effects of non-climatic events such as SSW is needed to anticipate future trends in mussel populations (Zippay & Helmuth, 2012).

4.3 | Predation effects on mussels

An aspect of the SSW outbreak not considered here is change in sea star population size structure, as sea star sizes were not measured. Elsewhere outside of Alaska, the loss of large sea stars and subsequent recruitment during recovery led to a shift in the size structure of the sea star populations to smaller mean size and biomass (Menge et al., 2016; Moritsch & Raimondi, 2018). We have not observed large recruitment events at our sites since the start of SSW, but small individuals have been observed since 2019 at KATM, KEFJ, and WPWS (e.g. *P. helianthoides* < 15 cm diameter, estimated size at five years old [Gravem et al., 2021]). Although *P. ochraceus* populations in much of Washington, Oregon, and California recovered in years following the SSW outbreak, their biomass, and therefore predation pressure, remained low (Moritsch & Raimondi, 2018). *Pisaster ochraceus* consumption rate and preferred prey size of *Mytilus trossulus* increases with sea star size (Gooding & Harley, 2015). While the small sea stars could still be significant predators of small mussels, the larger mussels may be safe from sea star predation for a few years

until post-SSW sea star recruits grow larger (although other mussel predators such as sea otters, sea ducks, and *Nucella* spp. snails are still present in the ecosystem). This could result in the recovery of predation pressure from sea stars lagging a few years behind the recovery in sea star density (Moritsch & Raimondi, 2018).

Predation by sea otters can affect mussel abundance and there is some recent evidence of sea otter diets shifting in response to changes in mussel availability. *Mytilus* spp. are a common prey item of sea otters throughout their range (Estes & Bodkin, 2002; Riedman & Estes, 1990), although their frequency of occurrence in sea otter diet can vary from miniscule (0.3% Calkins, 1978) to predominant (58%, Coletti et al., 2016) in the Gulf of Alaska. Mussels are abundant in spraint deposited during winter and spring in the Gulf of Alaska when mussels are gravid, while they become less frequent in direct observations of foraging sea otters usually obtained during summer months (Doroff et al., 2012; Doroff & Bodkin, 1994). In Glacier Bay, Alaska, sea otter diets became dominated by *M. trossulus* in 2018 and 2019 as mussel abundance increased in both the intertidal and subtidal (authors' personal observation). At our study sites, mussels were present in spraint at 47% in WPWS and > 80% in KEFJ and KBAY with little evidence of temporal trends between 2006–2019 (U.S. Geological Survey Alaska Science Center, National Park Service Southwest Alaska Inventory and Monitoring Network, & University of Alaska Fairbanks, 2022). However, at KATM prior to 2014, mussels were the predominant prey in about 10% of spraints compared to about 40% after 2014 (U.S. Geological Survey Alaska Science Center, National Park Service Southwest Alaska Inventory and Monitoring Network, & University of Alaska Fairbanks, 2022), suggesting an increase in consumption concurrent with the increase in mussel abundance we report here. These observations are consistent with a trophic cascade following declining sea stars through increased mussel abundance to increased mussel consumption by sea otters at KATM, where mussel increases were most evident.

Other mussel predators besides the three sea star species studied here and sea otters can have strong effects on mussel populations and will likely benefit from increased mussel abundance. Up to 81% of *M. trossulus* shells collected at a site in Kachemak Bay had drill holes, indicating predation by the whelk *Nucella lima* (Carroll & Highsmith, 1996). The small and cryptic sea stars, *Leptasterias* spp., can occur at high densities within mussel beds and can be abundant in Alaska (Chenelot et al., 2006; Paine, 1976) and consume smaller-sized prey, including mussels, than *P. ochraceus* (Menge, 1972). *Leptasterias hexactis* was impacted by SSW in California (Gravem & Morgan, 2017), but since *Leptasterias* spp. were not surveyed in the Gulf Watch Alaska long-term monitoring program, it is unknown how they were affected by SSW in Alaska. Throughout much of the eastern Pacific, birds including surfbirds (*Aphriza virgata*), gulls (*Larus glaucescens*, *L. occidentalis*), sea ducks such as Barrow's goldeneye (*Bucephala islandica*), and black oystercatchers (*Haematopus bachmani*) can derive a significant portion of their diet from mussels and affect mussel persistence (Marsh, 1986; Miller & Dowd, 2019; Robinson et al., 2018). Black oystercatchers also feed mussels to their chicks (O'Clair & O'Clair, 1998; Robinson et al., 2018) making mussels an important resource across black oystercatcher life stages. Sea ducks such as Barrow's goldeneyes consume primarily mussels and spend much of the winter near mussel beds (Esler et al., 2019). Surf scoters (*Melanitta perspicillata*) also consume large quantities of mussels and will use rocky intertidal mussel beds for foraging as mussels become depleted seasonally in other habitats, such as clam beds (Kirk et al., 2007).

5 | CONCLUSIONS

Effects of the changing sea star abundance and heatwaves on the nearshore ecosystem may differ globally depending on the dominant mussel species. *Mytilus trossulus* is a preferred prey compared to other *Mytilus* species it co-occurs with, including *Mytilus edulis* in the north Atlantic (Khaitov et al., 2018) and *Mytilus californianus* in the eastern Pacific (Menge et al., 1994). Mussel species that are better protected from sea star predation than *M. trossulus* by their thicker shells (Beaumont et al., 2008) and stronger defense responses (Lowen et al., 2013) may not respond as dramatically to decreased predation pressure from sea stars. From British Columbia to southern California, where *M. californianus* dominates and *M. trossulus* is typically only present at lower densities, *M. californianus* response to declines in sea stars was mixed, with expansion at some sites and no change in others (P. Raimondi, S. Gravem personal communication) and *M. californianus* cover decreased after the PMH (Miner et al., 2021).

Rocky intertidal ecosystems are shaped by a complex array of static (slope, substrate, etc.) and dynamic drivers (temperature, salinity, predation, etc.; Konar et al., 2019, Kunze et al., 2021), which can make understanding the causes of changes to abundance and distribution of species over space and time difficult. Long-term monitoring studies help to understand processes that affect rocky intertidal ecosystems because they can capture "natural experiments" such as the removal of sea stars over large spatial scales as seen here and other disturbance events like storms, heatwaves, and cold spells (Mieszkowska et al., 2021). The dynamics of foundational species such as mussels are particularly important as they influence community stability (Miner et al., 2021). As vital components of the nearshore food web, continued monitoring of mussels along with their predators, competitors, and environmental factors is needed to inform ecosystem-based management of nearshore species.

ACKNOWLEDGMENTS

The authors thank the volunteers, students, and researchers for their assistance in the field. We thank Alan Fukuyama, Alan Bennett, and Bill Thompson for their early contributions to the Gulf Watch intertidal monitoring program and Kimberly Kloecker for her work on data collection and processing. We thank Tim Shepherd (National Park Service) for maintaining databases of the Gulf Watch Alaska data and for his assistance with accessing data. We thank the crews of the Dreamcatcher, Waters, Island C, Ursa Major, and the Alaskan Gyre and the staff at the Kasitsna

Bay Laboratory for their support of field operations. We thank Rebecca Taylor (U.S. Geological Survey), Adam Smith (Quest Research Limited, Massey University, NZ), and Marti Anderson (Massey University, NZ) for advice on statistical analyses. We thank Vanessa von Biela (U.S. Geological Survey), Melissa Miner (UC Santa Cruz), and an anonymous reviewer for their reviews of the manuscript. Funding was provided in part by the *Exxon Valdez* Oil Spill Trustee Council. However, the findings and conclusions presented by the authors do not necessarily reflect the views or position of the Trustee Council. The scientific results and conclusions, as well as any views or opinions expressed herein, are those of the authors from NOAA and the Department of Commerce but do represent the views of the U.S. Geological Survey. Any use of trade, firm, or product names is for descriptive purposes only and does not imply endorsement by the U.S. Government.

CONFLICT OF INTEREST

We have no conflicts of interest.

DATA AVAILABILITY STATEMENT

The data use in this study are openly available through Gulf Watch Alaska data portal at gulfwatchalaska.org and the U.S. Geological Survey at: https://doi.org/10.5066/F7WH2N3T (temperature), https://doi.org/10.5066/F7513WCB (sea star density and mussel percent cover), and https://doi.org/10.5066/F7FN1498 (mussel density and mussel bed width).

ORCID

Sarah B. Traiger https://orcid.org/0000-0002-6222-1445
James L. Bodkin https://orcid.org/0000-0003-1641-4438
Heather A. Coletti https://orcid.org/0000-0001-9696-6093
Brenda Ballachey https://orcid.org/0000-0003-1855-9171
Daniel Esler https://orcid.org/0000-0001-5501-4555
Katrin Iken https://orcid.org/0000-0001-7961-1012
Brenda Konar https://orcid.org/0000-0002-8998-1612
Mandy R. Lindeberg https://orcid.org/0000-0002-8828-855X
Daniel Monson https://orcid.org/0000-0002-4593-5673
Brian Robinson https://orcid.org/0000-0001-8588-7162
Robert M. Suryan https://orcid.org/0000-0003-0755-8317
Benjamin P. Weitzman https://orcid.org/0000-0001-7559-3654

REFERENCES

Aarset, A. V. (1982). Freezing tolerance in intertidal invertebrates (a review). *Comparative Biochemistry and Physiology – Part A: Physiology*, *73*(4), 571–580. https://doi.org/10.1016/0300-9629(82)90264-X

Almada-Villela, P. C., Davenport, J., & Gruffydd, L. D. (1982). The effects of temperature on the shell growth of young *Mytilus edulis* L. *Journal of Experimental Marine Biology and Ecology*, *59*(2–3), 275–288. https://doi.org/10.1016/0022-0981(82)90121-6

Anderson, M., Gorley, R. N., & Clarke, K. R. (2008). PERMANOVA + for PRIMER user manual, 1: 1–218.

Bates, D., Maechler, M., Bolker, B., & Walker, S. (2015). Fitting linear mixed-effects models using lme4. *Journal of Statistical Software*, *67*(1), 1–48. https://doi.org/10.18637/jss.v067.i01

Beaumont, A. R., Hawkins, M. P., Doig, F. L., Davies, I. M., & Snow, M. (2008). Three species of *Mytilus* and their hybrids identified in a Scottish Loch: natives, relicts and invaders? *Journal of Experimental Marine Biology and Ecology*, *367*(2), 100–110. https://doi.org/10.1016/j.jembe.2008.08.021

Berlow, E. L. (1997). From canalization to contingency: Historical effects in a successional rocky intertidal community. *Ecological Monographs*, *67*(4), 435–460.

Blanchard, A., & Feder, H. M. (1997). Reproductive timing and nutritional storage cycles of *Mytilus trossulus* Gould, 1850, in Port Valdez, Alaska, site of a marine oil terminal. *Veliger*, *40*(2), 121–130.

Bodkin, J. L., Coletti, H. A., Ballachey, B. E., Monson, D. H., Esler, D., & Dean, T. A. (2018). Variation in abundance of Pacific Blue Mussel (*Mytilus trossulus*) in the Northern Gulf of Alaska, 2006–2015. *Deep-Sea Research Part II: Topical Studies in Oceanography*, *147*, 87–97. https://doi.org/10.1016/j.dsr2.2017.04.008

Bodkin, J. L., Dean, T. A., Coletti, H. A., & Ballachey, B. E. (2016). Mussel bed sampling, standard operating procedure – version 1.2, Southwest Alaska inventory and monitoring network.

Bourget, E. (1983). Seasonal variations of cold tolerance in intertidal mollusks and relation to environmental conditions in the St. Lawrence Estuary. *Canadian Journal of Zoology*, *61*(6), 1193–1201. https://doi.org/10.1139/z83-162

Brown, N. E. M., Therriault, T. W., & Harley, C. D. G. (2016). Field-based experimental acidification alters fouling community structure and reduces diversity. *Journal of Animal Ecology*, *85*, 1328–1339.

Buckley, B. A., Owen, M.-E., & Hofmann, G. E. (2001). Adjusting the thermostat: the threshold induction temperature for the heat-shock response in intertidal mussels (genus *Mytilus*) changes as a function of thermal history. *Journal of Experimental Biology*, *204*, 3571–3579.

Calkins, D. G. (1978). Feeding behavior and major prey species of the sea otter, *Enhydra lutris*, in Montague Strait, Prince William Sound Alaska. *Fishery Bulletin*, *76*(1), 125–131.

Carroll, M. L., & Highsmith, R. C. (1996). Role of catastrophic disturbance in mediating *Nucella-Mytilus* interactions in the Alaskan rocky intertidal. *Marine Ecology Progress Series*, *138*(1–3), 125–133. https://doi.org/10.3354/meps138125

Cerny-Chipman, E., Sullivan, J., & Menge, B. (2017). Whelk predators exhibit limited population responses and community effects following disease-driven declines of the keystone predator *Pisaster ochraceus*. *Marine Ecology Progress Series*, *570*, 15–28. https://doi.org/10.3354/meps12121

Chenelot, H., Iken, K., Konar, B., & Edwards, M. (2006). Spatial and temporal distribution of Echinoderms in rocky nearshore areas of Alaska. *NaGISA World Congress*, *8*, 11–28.

Coletti, H. A., Bodkin, J. L., Monson, D. H., Ballachey, B. E., & Dean, T. A. (2016). Detecting and inferring cause of change in an Alaska nearshore marine ecosystem. *Ecosphere*, *7*(10), 1–20.

Davenport, J., & Davenport, J. L. (2005). Effects of shore height, wave exposure and geographical distance on thermal niche width of intertidal fauna. *Marine Ecology Progress Series*, *292*, 41–50.

Dean, T. A., Bodkin, J. L., & Coletti, H. A. (2014). Protocol narrative for nearshore marine ecosystem monitoring in the Gulf of Alaska: version 1.1 Natural Resource Report.

Donahue, M. J., Desharnais, R. A., Robles, C. D., & Arriola, P. (2011). Mussel bed boundaries as dynamic equilibria: thresholds, phase shifts, and alternative states. *American Naturalist*, *178*(5), 612–625. https://doi.org/10.1086/662177

Doroff, A. M., Badajos, O., Corbell, K., Jenski, D., & Beaver, M. (2012). Assessment of sea otter (*Enhydra lutris kenyoni*) diet in Kachemak Bay, Alaska (2008–2010). *IUCN Otter Specialist Group Bulletin*, *29*(1), 15–23. https://doi.org/10.1017/CBO9781107415324.004

Doroff, A. M., & Bodkin, J. L. (1994). Sea otter foraging behavior and hydrocasssssrbon levels in prey. In T. R. Loughlin (Ed.), *Marine mammals and the Exxon Valdez* (pp. 193–207). Academic Press.

Esler, D., Bowman, T. D., Clair, C. E. O., Dean, T. A., Mcdonald, L. L., Waterbirds, S., International, T, Biology, W., Esler, D., Bowman, T. D., Clair, C. E. O., Dean, T. A., & Mcdonald, L. L. (2019). Densities of Barrow's Goldeneyes during winter in Prince William Sound, Alaska in relation to habitat, food and history of oil contamination. *Waterbirds: The International Journal of Waterbird Biology*, *23*(3), 423–429.

Estes, J. A., & Bodkin, J. L. (2002). Otters. In W. F. Perrin, B. Wursing, & J. G. M. Thewissen (Eds.), *Encyclopedia of marine mammals* (pp. 842–858). Academic Press.

Evans, W., Mathis, J. T., & Cross, J. N. (2014). Calcium carbonate corrosivity in an Alaskan inland sea. *Biogeosciences*, *11*(2), 365–379. https://doi.org/10.5194/bg-11-365-2014

Farrell, T. M. (1991). Models and mechanisms of succession: An example from a rocky intertidal community. *Ecological Monographs*, *61*(1), 95–113. https://doi.org/10.2307/1943001

Gazeau, F., Quiblier, C., Jansen, J. M., Gattuso, J.-P., Middelburg, J. J., & Heip, C. H. R. (2007). Impact of elevated CO_2 on shellfish calcification. *Geophysical Research Letters*, *34*(7), L07603. https://doi.org/10.1029/2006GL028554

Gooding, R. A., & Harley, C. D. G. (2015). Quantifying the effects of predator and prey body size on sea star feeding behaviors. *Biological Bulletin*, *228*(3), 192–200. https://doi.org/10.1086/BBLv228n3p192

Gravem, S.A., Heady, W. N., Saccomanno, V. R., Alvstad, K. F., Gehman, A. L. M., Frierson, T. N., & Hamilton, S. L. (2021). Pycnopodia helianthoides. IUCN Red List of Threatened Species.

Gravem, S. A., & Morgan, S. G. (2017). Shifts in intertidal zonation and refuge use by prey after mass mortalities of two predators. *Ecology*, *98*(4), 1006–1015. https://doi.org/10.1002/ecy.1672

Hamilton, S. L., Saccomanno, V. R., Heady, W. N., Gehman, A. L., Lonhart, S. I., Francis, F. T., Lee, L., Salomon, A. K., & Gravem, S. A. (2021). Disease-driven mass mortality event leads to widespread extirpation and variable recovery potential of a marine predator across the eastern Pacific. *Proceedings of the Royal Society B: Biological Sciences*, *288*, 20211195. 10/1098/rspb.2021.1195

Harley, C. D. G. (2008). Tidal dynamics, topographic orientation, and temperature-mediated mass mortalities on rocky shores. *Marine Ecology Progress Series*, *371*, 37–46.

Harley, J. R., Lanphier, K., Kennedy, E. G., Leighfield, T. A., Bidlack, A., Gribble, M. O., & Whitehead, C. (2020). The Southeast Alaska Tribal Ocean Research (SEATOR) Partnership: Addressing data gaps in harmful algal bloom monitoring and shellfish safety in Southeast Alaska. *Toxins*, *12*, 407.

Hemery, L. G., Marion, S. R., Romsos, C. G., Kurapov, A. L., & Henkel, S. K. (2016). Ecological niche and species distribution modelling of sea stars along the Pacific Northwest continental shelf. *Diversity and Distributions*, *22*(12), 1314–1327. https://doi.org/10.1111/ddi.12490

Herrlinger, T. J. (1983). *The diet and predator-prey relationships of the sea star Pycnopodia helianthoides (Brandt) from a central California kelp forest (Issue December)*. San Jose State University.

Hewson, I., Button, J. B., Gudenkauf, B. M., Miner, B., Newton, A. L., Gaydos, J. K., Wynne, J., Groves, C. L., Hendler, G., Murray, M., Fradkin, S., Breitbart, M., Fahsbender, E., Lafferty, K. D., Kilpatrick, A. M., Miner, C. M., Raimondi, P., Lahner, L., Friedman, C. S., … Harvell, C. D. (2014). Densovirus associated with sea-star wasting disease and mass mortality. *Proceedings of the National Academy of Sciences of the United States of America*, *111*(48), 17278–17283. https://doi.org/10.1073/pnas.1416625111

Hiebert, T. C. (2016). Mytilus trossulus. In T. C. Hiebert, B. A. Butler, & A. L. Shanks (Eds.), *Oregon estuarine invertebrates: Rudys' illustrated guide to common species* (3rd ed.). University of Oregon Libararies and Oregon Institute of Marine Biology.

IPCC (2019). Summary for policymakers. In H. O. Portner, D. C. Roberts, V. Masson-Delmotte, P. Zhai, M. Tignor, E. Poloczanska, K. Mintenbeck, A. Alegria, M. Nicolai, A. Okem, J. Petzold, B. Rama, & Wey (Eds.), *IPCC Special Report on the Ocean and Cryosphere in a Changing Climate*. IPCC.

Kay, S. W. C., Gehman, A.-L. M., & Harley, C. D. G. (2019). Reciprocal abundance shifts of the intertidal sea stars, *Evasterias troschelii* and *Pisaster ochraceus*, following sea star wasting disease. *Proceedings of the Royal Society B: Biological Sciences*, *286*(1901), 20182766. https://doi.org/10.1098/rspb.2018.2766

Khaitov, V., Makarycheva, A., Gantsevich, M., Lentsman, N., Skazina, M., Gagarina, A., Katolikova, M., & Strelkov, P. (2018). Discriminating eaters: Sea stars *Asterias rubens* L. Feed preferably on *Mytilus trossulus* Gould in mixed stocks of *Mytilus trossulus* and *Mytilus edulis* L. *Biological Bulletin*, *234*(2), 85–95. https://doi.org/10.1086/697944

Kirk, M. K., Esler, D., & Boyd, W. S. (2007). Foraging effort of Surf Scoters (*Melanitta perspicillata*) wintering in a spatially and temporally variable prey landscape. *Canadian Journal of Zoology*, *85*(12), 1207–1215. https://doi.org/10.1139/Z07-105

Konar, B., Iken, K., Coletti, H., Monson, D., & Weitzman, B. (2016). Influence of static habitat attributes on local and regional rocky intertidal community structure. *Estuaries and Coasts*, *39*(6), 1735–1745. https://doi.org/10.1007/s12237-016-0114-0

Konar, B., Mitchell, T. J., Iken, K., Coletti, H., Dean, T., Esler, D., Lindeberg, M., Pister, B., & Weitzman, B. (2019). Wasting disease and static environmental variables drive sea star assemblages in the Northern Gulf of Alaska. *Journal of Experimental Marine Biology and Ecology*, *520*(August), 1–10. https://doi.org/10.1016/j.jembe.2019.151209

Krylovich, O. A., Vasyukov, D. D., Khasanov, B. F., Hatfield, V., West, D., & Savinetsky, A. A. (2019). Hunter-gatherers subsistence and impact on fauna in the Islands of Four Mountains, Eastern Aleutians, Alaska, over 3000 yr. *Quaternary Research*, *91*(3), 983–1002.

Kunze, C., Wölfelschneider, M., & Rölfer, L. (2021). Multiple driver impacts on rocky intertidal systems: The need for an integrated approach. *Frontiers in Marine Science*, *8*(May), 1–13. https://doi.org/10.3389/fmars.2021.667168

Kurihara, H. (2008). Effects of CO_2-driven ocean acidification on the early developmental stages of invertebrates. *Marine Ecology Progress Series*, *373*, 275–284. https://doi.org/10.3354/meps07802

Lazo, C. S., & Pita, I. M. (2012). Effect of temperature on survival, growth and development of *Mytilus galloprovincialis* larvae. *Aquaculture Research*, *43*(8), 1127–1133. https://doi.org/10.1111/j.1365-2109.2011.02916.x

Lockwood, B. L., & Somero, G. N. (2011). Invasive and native blue mussels (genus *Mytilus*) on the California coast: The role of physiology in a biological invasion. *Journal of Experimental Marine Biology and Ecology*, *400*(1–2), 167–174. https://doi.org/10.1016/j.jembe.2011.02.022

Lowen, J. B., Innes, D. J., & Thompson, R. J. (2013). Predator-induced defenses differ between sympatric *Mytilus edulis* and *M. trossulus*. *Marine Ecology Progress Series*, *475*, 135–143. https://doi.org/10.3354/meps10106

Lubchenco, J., & Menge, B. A. (1978). Community development and persistnce in a low rocky intertidal zone. *Ecological Monographs*, *48*(1), 67–94.

Marsh, C. P. (1986). Rocky intertidal community organization: The impact of avian predators on mussel recruitment. *Ecology*, *67*(3), 771–786.

Mauzey, K. P., Birkeland, C., Dayton, P. K., & Summer, E. (1968). Feeding behavior of Asteroids and escape responses of their prey in the Puget Sound Region. *Feeding Behavior of Asteroids*, *49*(4), 603–619.

Melzner, F., Buchholz, B., Wolf, F., Panknin, U., & Wall, M. (2020). Ocean winter warming induced starvation of predator and prey: Winter warming starvation. *Proceedings of the Royal Society B:*

Biological Sciences, *287*(1931), 20200970. https://doi.org/10.1098/rspb.2020.0970rspb20200970

Menge, B. A. (1972). Competition for food between two intertidal starfish species and its effect on body size and feeding. *Ecology*, *53*(4), 635–644.

Menge, B. A., Berlow, E. L., Blanchette, C. A., Navarrete, S. A., Yamada, B., Monographs, S. E., & Aug, N. (1994). The keystone species concept: variation in interaction strength in a rocky intertidal habitat. *Ecological Monographs*, *64*(3), 249–286.

Menge, B. A., Cerny-Chipman, E. B., Johnson, A., Sullivan, J., Gravem, S., & Chan, F. (2016). Sea star wasting disease in the keystone predator *Pisaster ochraceus* in Oregon: Insights into differential population impacts, recovery, predation rate, and temperature effects from long-term research. *PLoS One*, *11*(5), e0153994. https://doi.org/10.1371/journal.pone.0153994

Mieszkowska, N., Burrows, M. T., Hawkins, S. J., & Sugden, H. (2021). Impacts of pervasive climate change and extreme events on rocky intertidal communities: Evidence from long-term data. *Frontiers in Marine Science*, *8*(May), 642764. https://doi.org/10.3389/fmars.2021.642764

Miller, L. P., & Dowd, W. W. (2019). Dynamic measurements of black oystercatcher (*Haematopus bachmani*) predation on mussels (*Mytilus californianus*). *Invertebrate Biology*, *138*(1), 67–73. https://doi.org/10.1111/ivb.12240

Miner, C. M., Burnaford, J. L., Ambrose, R. F., Antrim, L., Bohlmann, H., Blanchette, C. A., Engle, J. M., Fradkin, S. C., Gaddam, R., CDG, H., Miner, B. G., Murray, S. N., Smith, J. R., Whitaker, S. G., & Raimondi, P. T. (2018). Large-scale impacts of sea star wasting disease (SSWD) on intertidal sea stars and implications for recovery. *PLoS One*, *13*(3), e0192870.

Miner, C. M., Burnaford, J. L., Ammann, K., Becker, B. H., Fradkin, S. C., Ostermann-Kelm, S., Smith, J. R., Whitaker, S. G., & Raimondi, P. T. (2021). Latitudinal variation in long-term stability of North American rocky intertidal communities. *Journal of Animal Ecology*, *90*(9), 2077–2093. https://doi.org/10.1111/1365-2656.13504

Moritsch, M. M., & Raimondi, P. T. (2018). Reduction and recovery of keystone predation pressure after disease-related mass mortality. *Ecology and Evolution*, *8*(8), 3952–3964. https://doi.org/10.1002/ece3.3953

O'Clair, C. E., & Rice, S. D. (1985). Depression of feeding and growth rates of the seastar *Evasterias troschelii* during long-term exposure to the water-soluble fraction of crude oil. *Marine Biology*, *84*(3), 331–340. https://doi.org/10.1007/BF00392503

O'Clair, R. M., & O'Clair, C. E. (1998). *Southeast Alaska's rocky shores: Animals*. Plant Press.

O'Donnell, M. J., George, M. N., & Carrington, E. (2013). Mussel byssus attachment weakened by ocean acidification. *Nature Climate Change*, *3*(6), 587–590. https://doi.org/10.1038/nclimate1846

Olabarria, C., Gestoso, I., Lima, F. P., Vázquez, E., Comeau, L. A., Gomes, F., Seabra, R., & Babarro, J. M. F. (2016). Response of two Mytilids to a heatwave: The complex interplay of physiology, behaviour and ecological interactions. *PLoS One*, *11*(10), e0164330. https://doi.org/10.1371/journal.pone.0164330

Paine, R. T. (1974). Intertidal community structure – Experimental studies on the relationship between a dominant competitor and its principal predator. *Oecologia*, *15*(2), 93–120. https://doi.org/https://doi.org/10.1007/BF00345739

Paine, R. T. (1976). Size-limited predation: An observational and experimental approach with the Mytilus- Pisaster interaction. *Ecology*, *57*(5), 858–873.

Paul, A. J., & Feder, H. M. (1970). The food of the sea star *Pycnopodia helianthoides* (brandt) in Prince William Sound, Alaska. *Ophelia*, *14*(1–2), 15–22. https://doi.org/10.1080/00785236.1975.10421968

Rayssac, N., Pernet, F., Lacasse, O., & Tremblay, R. (2010). Temperature effect on survival, growth, and triacylglycerol content during the early ontogeny of *Mytilus edulis* and *M. trossulus*. *Marine Ecology Progress Series*, *417*, 183–191. https://doi.org/10.3354/meps08774

RCoreTeam. (2020). *R: A language and environment for statistical computing (R version 4.0.3 [2020-10-10])*. R Foundation for Statistical Computing. https://www.r-project.org/

Riedman, M. L., & Estes, J. A. (1990). The sea otter (*Enhydra lutris*): Behavior, ecology, and natural history. *Biological Report*, *90*(14), 1–126.

Robinson, B. H., Coletti, H. A., Phillips, L. M., & Powell, A. N. (2018). Are prey remains accurate indicators of chick diet? A comparison of diet quantification techniques for black oystercatchers. *Wader Study*, *125*(1), 20–32. https://doi.org/10.18194/ws.00105

Sanford, E. (1999). Regulation of keystone predation by small changes in ocean temperature. *Science*, *283*(5410), 2095–2097. https://doi.org/10.1126/science.283.5410.2095

Sanford, E. (2002). Water temperature, predation, and the neglected role of physiological rate effects in rocky intertidal communities. *Integrative and Comparative Biology*, *42*(4), 881–891. https://doi.org/10.1093/icb/42.4.881

Sewell, M. A., & Watson, J. C. (1993). A "source" for asteroid larvae?: recruitment of *Pisaster ochraceus*, *Pycnopodia helianthoides* and *Dermasterias imbricata* in Nootka Sound, British Columbia. *Marine Biology*, *117*(3), 387–398. https://doi.org/10.1007/BF00349314

Sousa, W. P. (1979). Disturbance in marine intertidal boulder fields: the nonequilibrium maintenance of species diversity. *Ecology*, *60*(6), 1225–1239.

Sousa, W. P. (1984). Intertidal mosaics: Patch size, propagule availability, and spatially variable patterns of succession. *Ecology*, *65*(6), 1918–1935.

Suchanek, T. H. (1992). Extreme biodiversity in the marine environment: Mussel bed communities of *Mytilus californianus*. *Northwest Environmental Journal*, *8*, 150–152.

Suchanek, T. H., & Seed, R. (1992). Population and community ecology of *Mytilus*. In E. Gosling (Ed.), *The mussel Mytilus: Ecology, physiology, genetics and culture* (pp. 87–170). Elsevier.

Suryan, R. M., Arimitsu, M. L., Coletti, H. A., Hopcroft, R. R., Lindeberg, M. R., Barbeaux, S. J., Batten, S. D., Burt, W. J., Bishop, M. A., Bodkin, J. L., Brenner, R., Campbell, R. W., Cushing, D. A., Danielson, S. L., Dorn, M. W., Drummond, B., Esler, D., Gelatt, T., Hanselman, D. H., … Zador, S. G. (2021). Ecosystem response persists after a prolonged marine heatwave. *Scientific Reports*, *11*(1), 1–17. https://doi.org/10.1038/s41598-021-83818-5

Tomanek, L., & Zuzow, M. J. (2010). The proteomic response of the mussel congeners *Mytilus galloprovincialis* and *M. trossulus* to acute heat stress: Implications for thermal tolerance limits and metabolic costs of thermal stress. *Journal of Experimental Biology*, *213*(20), 3559–3574. https://doi.org/10.1242/jeb.041228

U.S. Geological Survey, & National Park Service. (2022). Rocky intertidal data from Prince William Sound, Katmai National Park and Preserve, and Kenai Fjords National Park: U.S. Geological Survey data release. https://doi.org/10.5066/F7513WCB

U.S. Geological Survey Alaska Science Center, & National Park Service Southwest Alaska Inventory and Monitoring Network. (2022). Intertidal mussel (Mytilus) data from Prince William Sound, Katmai National Park and Preserve, and Kenai Fjords National Park (ver 2.0, July 2022): U.S. Geological Survey data release. https://doi.org/10.5066/F7FN1498

U.S. Geological Survey Alaska Science Center, National Park Service Southwest Alaska Inventory and Monitoring Network, & University of Alaska Fairbanks. (2022). Sea otter spraint data from Kachemak Bay, Katmai National Park and Preserve, Kenai Fjords National Park and Prince William Sound: U.S. Geological Survey data release. https://doi.org/10.5066/P9EDM6NL

U.S. Geological Survey Alaska Science Center, National Park Service Southwest Alaska Inventory and Monitoring Network, & University of Alaska Fairbanks College of Fisheries and Ocean Sciences.

(2022). Intertidal temperature data from Kachemak Bay, Prince William Sound, Katmai National Park and Preserve, and Kenai Fjords National Park (ver 2.0, July 2022): U.S. Geological Survey data release. https://doi.org/10.5066/F7WH2N3T

Walsh, J. E., Bieniek, P. A., Brettschneider, B., Euskirchen, E. S., Lader, R., & Thoman, R. L. (2017). The exceptionally warm winter of 2015/16 in Alaska. *Journal of Climate*, *30*(6), 2069–2088. https://doi.org/10.1175/JCLI-D-16-0473.1

Weitzman, B., Konar, B., Iken, K., Coletti, H., Monson, D., Suryan, R., Dean, T., Hondolero, D., & Lindeberg, M. R. (2021). Changes in rocky intertidal community structure during a marine heatwave in the northern Gulf of Alaska. *Frontiers in Marine Science*, *8*, 556820. https://doi.org/10.3389/fmars.2021.556820

White, R., Anderson, S., Booth, J., Braich, G., Draeger, C., Fei, C., Harley, C. D. G., Henderson, S., Jakob, M., Lau, C.-A., Admasu, L. M., Narinesingh, V., Rodell, C., Roocroft, E., Weinberger, K., & West, G. (2022). *The unprecedented Pacific northwest heatwave of June 2021 (Issue June)*. https://doi.org/10.21203/rs.3.rs-1520351/v1

Williams, R. J. (1970). Freezing tolerance in *Mytilus edulis*. *Comparative Biochemistry and Physiology*, *35*(1), 145–161. https://doi.org/10.1016/0010-406X(70)90918-7

Wootton, J. T. (1993). Size-dependent competition: effects on the dynamics vs. the end point of mussel bed succession. *Ecology*, *74*(1), 195–206.

Zippay, M. L., & Helmuth, B. (2012). Effects of temperature change on mussel. *Mytilus*. *Integrative Zoology*, *7*(3), 312–327. https://doi.org/10.1111/j.1749-4877.2012.00310.x

SUPPORTING INFORMATION

Additional supporting information can be found online in the Supporting Information section at the end of this article.

How to cite this article: Traiger, S. B., Bodkin, J. L., Coletti, H. A., Ballachey, B., Dean, T., Esler, D., Iken, K., Konar, B., Lindeberg, M. R., Monson, D., Robinson, B., Suryan, R. M., & Weitzman, B. P. (2022). Evidence of increased mussel abundance related to the Pacific marine heatwave and sea star wasting. *Marine Ecology*, *43*, e12715. https://doi.org/10.1111/maec.12715